

# Sharp ferroelectric phase transition in strained single-crystalline $\text{SrRuO}_3/\text{Ba}_{0.7}\text{Sr}_{0.3}\text{TiO}_3/\text{SrRuO}_3$ capacitors

R. Dittmann,<sup>a)</sup> R. Plonka,<sup>b)</sup> E. Vasco, N. A. Pertsev,<sup>c)</sup> J. Q. He, C. L. Jia, S. Hoffmann-Eifert, and R. Waser

*Institut für Festkörperforschung and Center of Nanoelectronic Systems for Information Technology, Forschungszentrum Jülich, D-52425 Jülich, Germany*

(Received 11 August 2003; accepted 17 October 2003)

Single-crystalline all-perovskite  $\text{SrRuO}_3/\text{Ba}_{0.7}\text{Sr}_{0.3}\text{TiO}_3/\text{SrRuO}_3$  thin-film capacitors epitaxially grown on  $\text{SrTiO}_3$  exhibit a sharp paraelectric-to-ferroelectric phase transition at 350 K with a maximum permittivity of about 6660. This value is comparable to that of bulk ceramics and exceeds by several times the highest values reported for  $\text{Ba}_{0.7}\text{Sr}_{0.3}\text{TiO}_3$  thin film capacitors. The observed thickness dependence of the dielectric response is analyzed with the aid of a thermodynamic theory. It is shown that a weak decrease of the permittivity with the  $\text{Ba}_{0.7}\text{Sr}_{0.3}\text{TiO}_3$  thickness decreasing from 200 to 10 nm can be explained solely by the thickness-dependent strain relaxation in epitaxial films without assuming the presence of low-permittivity layers at the film/electrode interfaces.

© 2003 American Institute of Physics. [DOI: 10.1063/1.1633027]

In view of a high permittivity displayed in the bulk form,<sup>1,2</sup>  $\text{Ba}_{0.7}\text{Sr}_{0.3}\text{TiO}_3$  (BST 70/30) represents a promising candidate as a dielectric material to be used in new generations of dynamic random access memory (DRAM) cells.<sup>3</sup> Most of the work on BST thin films, however, has been performed on Pt/Si substrates.<sup>3–5</sup> In this case, the ferroelectric phase transition in BST thin films is suppressed due to their polycrystalline structure and in-plane tensile strains induced by a thick Si substrate. As a result, the BST dielectric constant is reduced in these films by about at least one order of magnitude with respect to the bulk value, and no ferroelectric phase is observed. In order to eliminate grain-size effects, several groups have investigated single-crystalline BST films.<sup>6–9</sup> The highest measured dielectric response of these films is around 1000.<sup>6</sup> Depending on the film quality, BST films may show the paraelectric to ferroelectric phase transition, but much broader than that in a bulk material.

Another drawback to the incorporation of BST films in DRAM devices is a strong decrease of the observed dielectric response with decreasing film thickness which is usually attributed to the existence of low-permittivity layers at the film–electrode interfaces.<sup>4</sup> In most of the performed investigations, the capacitors involved metallic top electrodes.<sup>10,11</sup> All-perovskite  $\text{SrRuO}_3/\text{BST}/\text{SrRuO}_3$  capacitors have been investigated only with polycrystalline  $\text{SrRuO}_3$  (SRO) top electrodes.<sup>8</sup> We are not aware of detailed studies of the thickness effect on the dielectric properties of BST films stacked symmetrically between two epitaxial oxide electrodes, which will be presented in this letter and are necessary to draw conclusions about the existence of a “dead layer” at that kind of interface.

Thin-film capacitors were fabricated on single-crystalline (100)  $\text{SiTiO}_3$  (STO) substrates. The SRO/BST/SRO heterostructures were grown *in-situ* by pulsed laser deposition (PLD), employing a KrF excimer laser with an energy density of 5 J/cm<sup>2</sup> and a frequency of 10 Hz. First, a 100-nm-thick bottom layer of SRO was deposited at 775 °C with an oxygen pressure of 0.25 mbar. Subsequently, the BST film was grown on SRO at 680 °C and the same oxygen pressure. The BST film thickness has been varied between 10 and 200 nm. Finally, the BST film was covered with a 30-nm-thick SRO top electrode deposited at the conditions indicated above for BST.

The high-quality cube-on-cube epitaxial relationship of BST/SRO on STO was proved by x-ray diffraction (XRD)  $\varphi$ -scan measurements and rocking curves with a full width at half-maximum of 0.05°. High-resolution transmission electron microscopy (TEM) investigations of the SRO/BST/SRO heterostructures showed sharp BST/SRO interfaces. No secondary phases could be detected. In the heterostructures with a BST thickness of 9 nm, no misfit dislocations were observed [Fig. 1(a)]. In the 17-nm-thick BST layer, misfit dislocations were found to appear at a distance of a few nanometers away from the bottom interface [Fig. 1(b)]. In Fig. 1(b), the vertical arrow marks a dislocation.

Thin-film capacitors were fabricated by patterning the SRO top electrodes by optical lithography and Ar-ion-beam etching.

Figure 2 shows the temperature dependence of the dielectric response  $\epsilon_{\text{eff}}$  of the SRO/200-nm-BST/SRO capacitors performed at 10 kHz. The presence of a strong dielectric peak with the maximum permittivity  $\epsilon_{\text{max}} \approx 6660$  indicates a sharp paraelectric-to-ferroelectric phase transition at the transition temperature  $T_c \approx 350$  K. This transition is confirmed by the results of polarization hysteresis measurements, which demonstrate that, at temperatures below 350 K, a nonzero remnant polarization  $P_r$  appears in BST films, reaching values as high as  $P_r \approx 14 \mu\text{C}/\text{cm}^2$  at  $T = 200$  K (see the inset in Fig. 2). It should be noted that  $T_c$  is around 40 K higher than

<sup>a)</sup> Author to whom correspondence should be addressed; electronic mail: r.dittmann@fz-juelich.de

<sup>b)</sup> Permanent address: Institut für Werkstoffe der Elektrotechnik, RWTH Aachen University of Technology, 52056 Aachen, Germany.

<sup>c)</sup> Permanent address: A. F. Ioffe Physico-Technical Institute, Russian Academy of Sciences, 194021 St. Petersburg, Russia; electronic mail: pertsev@domain.ioffe.rssi.ru

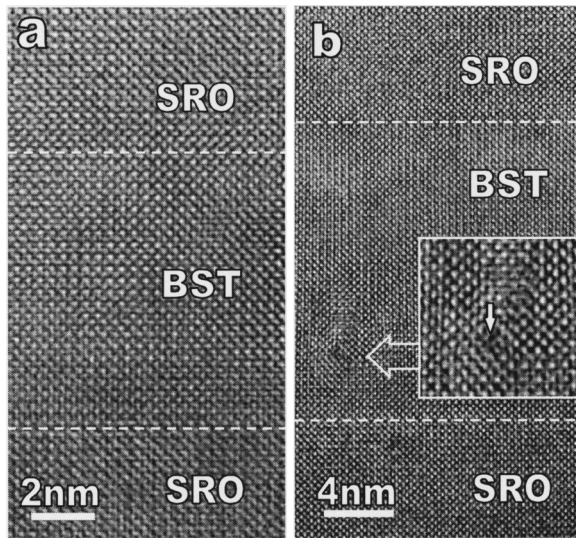


FIG. 1. Lattice fringe images of two SRO/BST/SRO heterostructures deposited on STO and involving 9-nm-thick (a) and 17-nm-thick (b) BST layers. The dashed lines denote the interfaces, and the vertical arrow marks a misfit dislocation in the 17-nm-thick BST layer.

that of the bulk BST 70/30 ceramic.<sup>1</sup> The maximum permittivity  $\epsilon_{\max} \approx 6660$  is in the same order of magnitude as values reported for bulk ceramics.<sup>1,2</sup>

Figure 3 shows the variation of the inverse capacitance density  $c_{\text{eff}}^{-1}$  for thicknesses  $H$  ranging from 10 to 200 nm. The observed linear dependence with a nonzero intercept  $A/C(H \rightarrow 0)$  is similar to the one reported for Pt/BST/Pt capacitors.<sup>4</sup> However, the apparent “interfacial” capacitance  $c_i = c_{\text{eff}}(H \rightarrow 0) \approx 1 \text{ F/m}^2$  is much larger than the capacitances determined in Ref. 4 ( $c_i = 0.117 \text{ F/m}^2$ ) and Ref. 11 ( $c_i = 0.022 \text{ F/m}^2$ ) for Pt/BST/Pt and SRO/BST/Au structures, respectively. The estimated permittivity  $\epsilon_{\infty} \approx 6600$  of an infinitely thick BST film, which can be extracted from the slope in Fig. 3, is also very large in comparison with  $\epsilon_{\infty} \approx 1000$  for SRO/BST/Au capacitors.<sup>11</sup> The main distinction of our BST capacitors from those studied earlier is that they are fully epitaxial trilayers.

The out-of-plane lattice constant  $c$  of BST films was determined from the 002 XRD peak. It was found that this lattice parameter increases markedly in the thinnest films (Fig. 3). This fact indicates the presence of thickness-dependent lattice strains in our BST films. Therefore, the strain effect on the dielectric properties of epitaxial BST films was analyzed theoretically. The in-plane lattice strains  $S_1$  and  $S_2$  in a ferroelectric film are equal to the nominal misfit strain  $S_m^0 = (b - a_0)/a_0$  in an epitaxial couple, only in the absence of plastic relaxations ( $a_0$  is the lattice constant of a freestanding film and  $b$  is the in-plane lattice parameter of the bottom electrode strained by a thick substrate). If the film thickness  $H$  exceeds a critical value  $H_c$ , above which the introduction of misfit dislocations is energetically favorable,<sup>12</sup> the lattice strains  $S_1 = S_2 = S_m$  become thickness dependent. When the dislocation density  $\rho \ll 1$ , the actual misfit strain can be evaluated as  $S_m = (b^* - a_0)/a_0$ , where  $b^* = b(1 - \rho)$  is the effective lattice parameter of the bottom electrode.<sup>13,14</sup> It is widely accepted that the generation of misfit dislocations in perovskites occurs only at the growth temperature because the dislocation glide is suppressed at

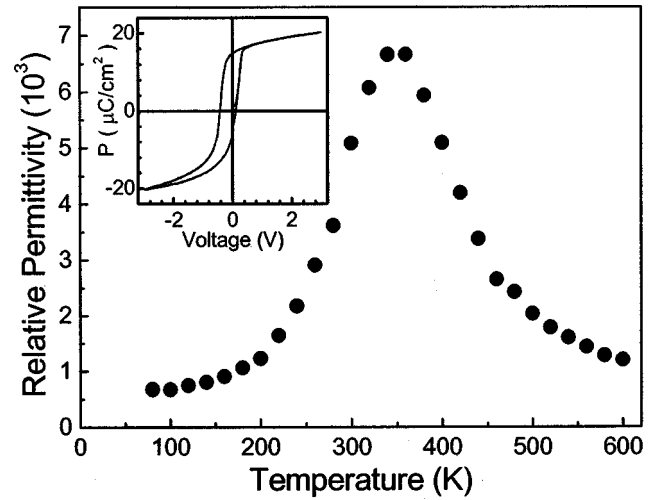


FIG. 2. Dielectric response of the 200-nm-thick epitaxial BST film as a function of temperature. The inset shows the polarization versus voltage hysteresis loop measured at 200 K on the same sample recorded at 100 Hz.

lower temperatures due to the relatively high Peierls barriers. Using the results of Ref. 12, for the density  $\rho(H)$  of misfit dislocations at the film/electrode interface, we obtain  $\rho(H) \approx \eta S_m^0(T_g)(1 - H_c/H)$ , where the factor  $\eta \leq 1$  allows for partial suppression of the dislocation generation due to kinetic reasons. Hence, the thickness dependence of the misfit strain at  $H > H_c$  can be written as

$$S_m(T, H) = S_m^{\infty}(T) + \eta S_m^0(T_g) \frac{H_c}{H}. \quad (1)$$

Here  $S_m^{\infty}(T) = S_m^0(T) - \eta S_m^0(T_g)$  represents the in-plane strains in a very thick fully relaxed film ( $H \gg H_c$ ).

According to the nonlinear thermodynamic theory,<sup>16–18</sup> the lattice strain  $S_3$  in the thickness direction of a tetragonal ferroelectric film (stable under compressive stress at  $S_m < 0$ ) can be calculated as  $S_3 = 2s_{12}S_m/(s_{11} + s_{12}) + [Q_{11} - 2s_{12}Q_{12}/(s_{11} + s_{12})]P_3^2$ , where  $s_{ln}$  are the elastic compli-

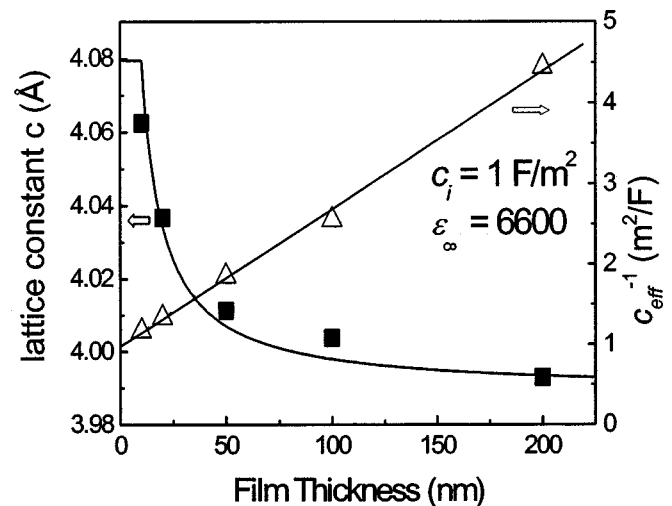


FIG. 3. Thickness dependence of the out-of-plane lattice constant (left vertical axis) and the inverse of the capacitance density (right vertical axis). Squares represent the out-of-plane lattice constants  $c(H)$  of epitaxial BST films determined by x-ray diffraction. The solid curve shows the theoretically calculated dependence  $c(H)$ . The triangles represent the inverse capacitance density of single-crystalline SRO/BST/SRO capacitors. The solid line is a linear fit to the experimental data points.

ances at constant polarization,  $Q_{1n}$  are the electrostrictive constants in polarization notation, and  $P_3$  the out-of-plane polarization.<sup>19</sup> Using the above relations together with Eq. (1), the dependence  $c(H) = a_0(1 + S_3)$  for BST 70/30 films at room temperature was calculated.<sup>20</sup> The results are shown in Fig. 3 together with the measured values of the lattice parameter  $c(H)$ . Good agreement between theoretical and experimental results support the validity of Eq. (1) in our films.

Now we can calculate the thickness dependence of the film permittivity that originates in the strain effect. As shown by Pertsev *et al.*,<sup>21</sup> the misfit-strain dependence of the relative out-of-plane permittivity  $\epsilon_{33}$  obeys the Curie–Weiss-type law:  $\epsilon_{33}(S_m) = K_s / (S_m^* - S_m)$ . In this equation, which is written for a tetragonal film grown on a compressive substrate ( $S_m < 0$ ) and valid at  $S_m < S_m^*$  only,  $K_s = -(s_{11} + s_{12}) / (8\epsilon_0 Q_{12})$  is the material parameter governing the strain sensitivity of dielectric response, and  $S_m^*(T) = a_1(T) \times (s_{11} + s_{12}) / (2Q_{12})$  is the critical misfit strain, which makes the prototypic phase unstable with respect to appearance of the out-of-plane polarization  $P_3$ . The substitution of Eq. (1) into the above relation gives at  $H > H_c$ ,

$$\frac{1}{\epsilon_{33}(T, H)} = \frac{1}{\epsilon_{33}^\infty(T)} - \frac{\eta S_m^0(T_g) H_c}{K_s H}, \quad (2)$$

where  $\epsilon_{33}^\infty(T) = K_s / [S_m^*(T) - S_m^\infty(T)]$  is the permittivity of a very thick strained film ( $H \gg H_c$ ). Equation (2) shows that the inverse of film permittivity is a linear function of  $H^{-1}$ .

The intrinsic dielectric response of a ferroelectric film given by Eq. (2) cannot be measured directly. Indeed, the dielectric measurements may include intrinsic or extrinsic low-permittivity layers at the film/electrode interfaces. If the thickness of these layers is much smaller than the film thickness, we obtain from Eq. (2)

$$\frac{1}{c_{\text{eff}}} = \frac{1}{c_i} - \frac{\eta S_m^0(T_g) H_c}{\epsilon_0 K_s} + \frac{H}{\epsilon_0 \epsilon_{33}^\infty}. \quad (3)$$

Two important results follow from Eq. (3): (i) the slope of the dependence  $c_{\text{eff}}^{-1}(H)$  reflects the permittivity  $\epsilon_{33}^\infty$  of a thick strained film, but not of the bulk material; and (ii) a considerable nonzero intercept is obtained even when the interface effect is negligible. Numerical estimates show that the second term in Eq. (3) can be as large as several  $\text{m}^2/\text{F}$ . Therefore, the nonzero intercept in Fig. 3 may be explained solely by the strain-related thickness dependence of the intrinsic permittivity of BST films.

Finally, it must be stressed that the increase of  $T_c$  in our 200-nm-thick BST film can be explained by the strain effect as well. Indeed, the thermodynamic theory<sup>15</sup> predicts  $T_c = \theta + S_m(T_c) 4\epsilon_0 C Q_{12} / (s_{11} + s_{12})$ , where  $\theta$  and  $C$  are the

Curie–Weiss temperature and constant of the bulk material, respectively. Taking  $\theta = 290$  K,  $C = 1.18 \times 10^5$  (Ref. 1) and  $S_m(T_c) \approx -2 \times 10^{-3}$  (since  $S_m$  weakly depends on temperature in our case), we obtain  $T_c \approx 360$  K, in good agreement with the measurements.

<sup>1</sup>A. D. Hilton and B. W. Ricketts, J. Phys. D **29**, 1321 (1996).

<sup>2</sup>G. A. Smolenski and K. S. Rogatschev, Zh. Tekh. Fiz. **27**, 1753 (1954).

<sup>3</sup>D. E. Kotecki, J. D. Baniecki, H. Shen *et al.*, IBM J. Res. Dev. **43**, 367 (1999).

<sup>4</sup>C. Basceri, S. K. Streiffer, A. I. Kingon, and R. Waser, J. Appl. Phys. **82**, 2497 (1997); T. R. Taylor, P. J. Hansen, B. Acikel, N. Pervez, R. A. York, S. K. Streiffer, and J. S. Speck, Appl. Phys. Lett. **80**, 1978 (2002); M. A. McCormick, R. K. Roeder, and E. B. Slamovich, J. Mater. Res. **16**, 1200 (2001).

<sup>5</sup>S. K. Streiffer, C. Basceri, C. B. Parker, S. E. Lash, and A. I. Kingon, J. Appl. Phys. **86**, 4565 (1999).

<sup>6</sup>K. Abe and S. Komatsu, J. Appl. Phys. **77**, 6461 (1995).

<sup>7</sup>Q. X. Jia, X. D. Wu, S. R. Foltyn, and P. Tiwari, Appl. Phys. Lett. **66**, 2197 (1995).

<sup>8</sup>M. Izuha, K. Abe, and N. Fukushima, Jpn. J. Appl. Phys. **36**, 5866 (1997); K. Abe, N. Yanase, S. Komatsu, K. Sano, N. Fukushima, and T. Kawabuko, IEICE Trans. Electron. **E81-C**, 505 (1998).

<sup>9</sup>C. M. Chu and P. Lin, Appl. Phys. Lett. **72**, 1241 (1998).

<sup>10</sup>C. S. Hwang, J. Appl. Phys. **92**, 432 (2002).

<sup>11</sup>L. J. Sinnamon, R. M. Bowman, and J. M. Gregg, Appl. Phys. Lett. **78**, 1724 (2002); **81**, 889 (2002).

<sup>12</sup>J. Matthews and A. E. Blakeslee, J. Cryst. Growth **27**, 118 (1974).

<sup>13</sup>J. S. Speck and W. Pompe, J. Appl. Phys. **76**, 466 (1994).

<sup>14</sup>Z.-G. Ban and S. P. Alpay, J. Appl. Phys. **93**, 504 (2003).

<sup>15</sup>The quantities involved in Eq. (1) were estimated as  $S_m^0(T_g = 973 \text{ K}) \approx -15 \times 10^{-3}$ ,  $S_m^0(T = 300 \text{ K}) \approx -12 \times 10^{-3}$ ,  $H_c \approx 10 \text{ nm}$ , and  $\eta \approx 0.7$ . The strains were calculated using the data of lattice constants and thermal expansion coefficients of BaTiO<sub>3</sub>, SrTiO<sub>3</sub>, and SRO [Landolt–Börnstein, Numerical Data and Functional Relationships in Science and Technology, New Series, Vol. III/29a (Springer, Berlin, 1992); Y. S. Touloukian, R. K. Kirby, R. E. Taylor, and T. Y. R. Lee, Thermal Expansion Nonmetallic Solids, Thermophysical Properties of Matter (Plenum, New York, 1997), Vol. 13. The kinetic factor  $\eta$  was determined using the experimental value of  $S_m = (a - a_0) / a_0 \approx -2 \times 10^{-3}$ , which was evaluated from the measured in-plane lattice constant  $a \approx 0.397 \text{ nm}$  of the 200-nm-thick BST film and the estimated prototypic-cell size  $a_0(T = 300 \text{ K}) \approx 0.3977 \text{ nm}$ .

<sup>16</sup>N. A. Pertsev, A. G. Zembilgotov, and A. K. Tagantsev, Ferroelectrics **223**, 79 (1999).

<sup>17</sup>N. A. Pertsev, A. K. Tagantsev, and N. Setter, Phys. Rev. B **61**, R825 (2000).

<sup>18</sup>N. A. Pertsev, V. G. Kukhar, H. Kohlstedt, and R. Waser, Phys. Rev. B **67**, 054107 (2003).

<sup>19</sup> $P_3$  may be evaluated from the relation  $P_3^2 = -a_3^*/2a_{33}^*$ , where  $a_3^* = a_1 - S_m 2Q_{12} / (s_{11} + s_{12})$  and  $a_{33}^* = a_{11} + Q_{12}^2 / (s_{11} + s_{12})$ ,  $a_1$  and  $a_{11}$  being the dielectric stiffness and second-order stiffness coefficient at constant stress. We employ the  $P^4$  approximation to calculate the polarization of epitaxial BST 70/30 films because the phase transition in these films must be of the second order (Ref. 15).

<sup>20</sup>The following values were used:  $a_1 = 3.83 \times 10^6 \text{ m/F}$  (evaluated from the data given in Ref. 1),  $a_{11} = 1.767 \times 10^8 \text{ m}^5/\text{C}^2\text{F}$ ,  $s_{11} = 5.9 \times 10^{-12} \text{ m}^2/\text{N}$ ,  $s_{12} = -1.9 \times 10^{-12} \text{ m}^2/\text{N}$ ,  $Q_{11} = 0.10 \text{ m}^4/\text{C}^2$ , and  $Q_{12} = -0.0346 \text{ m}^4/\text{C}^2$  (calculated by linear interpolation of the BaTiO<sub>3</sub> and SrTiO<sub>3</sub> parameters given in Refs. 16 and 17).

<sup>21</sup>N. A. Pertsev, V. G. Koukhar, R. Waser, and S. Hoffmann, Appl. Phys. Lett. **77**, 2596 (2000).